Beyond decentralized wafer/reticle stage control design: a double-Youla approach for enhancing synchronized motion

Control Engineering Practice 83 (2019) 21–32

Contents lists available at ScienceDirect

Control Engineering Practice

journal homepage: www.elsevier.com/locate/conengprac

Beyond decentralized wafer/reticle stage control design: A double-Youla approach for enhancing synchronized motion

Enzo Evers [a,*], Marc van de Wal [b], Tom Oomen [a]

[a] Department of Mechanical Engineering, Eindhoven University of Technology, 5600 MB Eindhoven, The Netherlands
[b] ASML Netherlands, De Run 6501, 5504 DR, Veldhoven, The Netherlands

ARTICLE INFO

Keywords:
Mechatronic systems
Motion control systems
Decentralized control
Coupling
Youla–Kucera parameterization
Systems-of-systems

ABSTRACT

Industrial wafer scanners often consists of multiple subsystems. Traditionally, these systems-of-systems are divided into manageable subproblems at the expense of the overall performance, that is determined by the synchronicity of the motions of the subsystems. The aim of this paper is to enhance overall system performance by posterior coupling of the controlled subsystems. A framework that relates to the Youla parameterization is developed that connects the additional control elements affinely to the overall system performance criterion. The resulting framework parametrizes all stabilizing bidirectional coupling controllers, and enables improved performance. Robust stability is subsequentially addressed through a double-Youla approach. Application to a wafer scanner confirms superior performance of the joint wafer stage and reticle stage performance, while maintaining full system robust stability.

1. Introduction

Many mechatronic systems in the manufacturing industry consist of multiple subsystems that jointly contribute to achieve a certain overall performance. Examples of such systems-of-systems include wafer scanners used in the lithographic industry (Butler, 2011), where the wafer stage and reticle stage synchronization is critical to achieve the required overlay performance; gantry and carriage platforms such as large scale industrial printers (Bolder, 2015), where performance of both subsystems is directly related to the print quality; and roll-to-roll processing plants, where synchronization between rolls is required for correct deposition of the layer material (Chen, He, Zheng, Song, & Deng, 2016). In all these cases, the relative positioning of the subsystems defines the overall system performance.

The design and control of these systems-of-systems is traditionally divided into tractable subproblems with error budgets (Jabben, Trumper, & Eijk, 2008). Typically, the subsystems aim at a certain absolute positioning accuracy, together these then imply good relative positioning of the subsystems. The main reason is that the overall design problem is too complex to be handled by manual controller design. In fact, already for a single multivariable subsystem a centralized design often is too complex (Oomen, 2018), and by far, the majority of the industrial control systems are still controlled by traditional decentralized PID controllers. Veritably, typical motion control guidelines in Oomen (2018) reveal that control performance and modeling effort should be well-balanced, typically leading to PID controllers by utilizing decentralized controller structures and non-parametric frequency response functions.

In the typical case where the control design is divided into manageable subproblems, the overall performance of the system is limited by the worst-case performance of the subsystems. In turn, the worst case performance is determined by the performance limitations associated with the individual subsystems (Seron, Braslavsky, & Goodwin, 1997). Typically, these subsystems are scalar or at least controlled in decentralized loops using a local performance measure. This is commonly done to facilitate decentralized design, where each module is designed and controlled using its own specifications and error budget. This decomposition of the overall system leads to newly introduced performance limitations. For instance, the definition of Single-In–Single-Out (SISO) subsystems leads to new zeros, which can be non-minimum phase and directly introduce performance limitations. Indeed, this introduction of zeros is well-known and well-understood from squaring down (Maciejowski, 1989). In sharp contrast, the full system using an overall performance criterion often has much less performance variables compared to the number of inputs, in which case the overall system using the global performance criterion generally does not exhibit these NMP zeros. Indeed, non-square systems generally have no such performance limiting zeros (Freudenberg, Hollot, Middleton, & Toochinda, 2003; van Zundert, Luijten, & Oomen, 2018), and hence exploiting the freedom in the controller architecture in conjunction with the overall performance goal may alleviate traditional performance limitations.

The aim of this paper is to improve the combined system performance while maintaining the original decentralized design and control

* Corresponding author.
E-mail address: e.evers@tue.nl (E. Evers).

https://doi.org/10.1016/j.conengprac.2018.10.011
Received 29 August 2017; Received in revised form 8 October 2018; Accepted 9 October 2018
Available online xxxx
0967-0661/

structure. This allows for superior performance in the overall performance criterion, while maintaining the original controller design approach for the controlled variables. This is achieved by: (1) additional add-on coupling elements to the existing decentralized control structure, and (2) optimizing these control elements for a full system performance criterion.

The potential and industrial acceptance of add-on controller extensions has been confirmed in several preliminary ad hoc experimental studies. Research examples of improved synchronization by advanced feedforward can be found in Navarrete, Heertjes, and Schmidt (2015), see also Boeren, Bruijnen, van Dijk, and Oomen (2014) for related feedforward results. In Barton and Alleyne (2007) and Mishra, Yeh, and Tomizuka (2008) improved synchronization is achieved by using iterative learning control. Rational filters are used in direct feedback of the relative error in Wang, Yin, and Duan (2006). Typically, in these experimental studies the controller is extended by a one-way coupling. Such unidirectional interaction is also considered in Sakata and Fujimoto (2009) using rational filters and Heertjes and Temizer (2012) using data-based optimization of FIR filters. Bidirectional interaction allows for inherently better performance due to a larger design freedom. However, bidirectional coupling affects closed-loop stability (Skogestad & Postlethwaite, 2009), which is not the case for unidirectional coupling.

Although several attempts to improve overall system performances have been made, at present no systematic framework is available for the design of bidirectional controller coupling that is applicable to synchronized motion control. In this paper the potential enhancement is shown through fundamental analysis and a generalized framework is developed that achieves this performance gain by connecting the add-on controller elements to the true performance criterion.

The main contribution of this paper is a control design for coupling in decentralized controllers which is illustrated on a highly complex, high performance motion system. The following sub-contributions are identified.

- C1 A framework that facilitates systematic design and analysis of nominal add-on coupling filters to achieve improved overall system performance. In addition, it encompasses all present approaches outlined above as a special case.
- C2 Design guidelines for coupling filter synthesis, suitable for both norm-optimal ($\mathcal{H}_2, \mathcal{H}_\infty$) design and manual tuning, where the latter facilitates industrial implementation (van de Wal, van Baars, Sperling, & Bosgra, 2002).
- C3 An extension that appropriately addresses robust stability by considering model uncertainty bounds.
- C4 A case study of an industrial wafer scanner is presented, where both nominal performance and robust performance are investigated.

In Evers, van de Wal, and Oomen (2017), a preliminary version addressing in part C1, C2 is presented. The present paper extends this to a more general setting containing more detailed proofs and explanation, and, in addition, C3, C4. Research related to results presented here includes Barton and Alleyne (2007), Heertjes and Temizer (2012), Lambregts, Heertjes, and van der Veek (2015), Navarrete et al. (2015) and Sakata and Fujimoto (2009).

The framework guarantees robust stability under uncertainty in the system dynamics, finite accuracy of the plant model and neglected subsystem interaction components. The presented framework provides a systematic design based on several Youla-type parameterizations that in turn depend on coprime factorizations. The approach relates to coprime factorization based Youla result in Tay, Mareels, and Moore (1998), see also Chen, Jiang, and Tomizuka (2015) and Oomen, van der Maas, Rojas, and Hjalmarsson (2014b). The proposed framework provides a basis for general control design methodologies ranging from manual tuning to $\mathcal{H}_2/\mathcal{H}_\infty/\mu$-based optimal control. For clarity and brevity of the exposition the framework is presented for a 2×2 SISO case. The framework can directly applied to MIMO systems along conceptually similar lines. Moreover, it is assumed that the contribution of the additional coupling controllers to the actuator signal is relatively small. For the considered wafer scanner application, this assumption is valid, the control input predominantly consists of feedforward inputs (de Gelder, van de Wal, Scherer, Hol, & Bosgra, 2006). Therefore, non-linear effects such as dead-zones, saturation, and anti-windup (Prempain, Turner, & Postlethwaite, 2009) are considered beyond the scope of this paper.

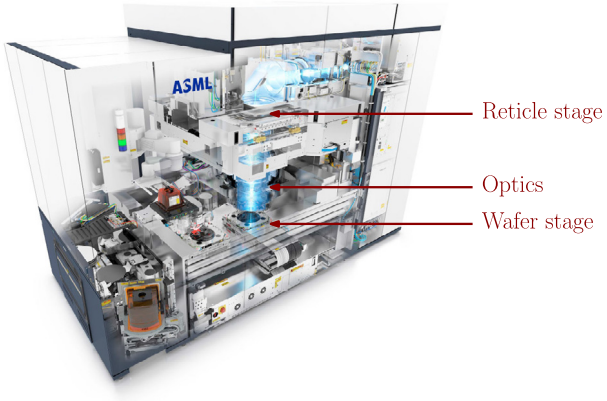

Fig. 1. Artist impression of a wafer scanner, an industrial production machine used in the lithographic industry.

2. Motivation and problem formulation

In this section, the problem considered in this paper is formulated. First, a motivating case study is presented, followed by the specification of the requirements and control goal.

2.1. Industrial wafer scanner: the role of reticle stage and wafer stage

The potential performance benefit of the additional controller freedom due to the coupling elements is exploited in an industrial case study. The following section presents the considered system, the industrial context and the control challenges.

The case study considered in this paper is an industrial waferscanner, as shown in Fig. 1. A waferscanner is used in the lithographic step in the production process of integrated circuits. An abstract representation of the considered moving stages, the reticle stage and wafer stage, is shown in Fig. 2.

During the exposure step of the lithographic process, light, typically with a wavelength of approximately 14 nm in state-of-the-art equipment, travels from a source, located outside the machine, through the reticle. The reticle contains the image of the to be produced IC and the beam is projected through the optical column onto a light-sensitive layer on the wafer. The illuminated photoresist is subsequently removed using a chemical solvent. Further chemical processing enable etching of the exposed patterns, which is repeated for each subsequent layer. Approximately 20 layers are required to form each wafer. The final wafer, a silicon disk with a diameter of 300 mm, contains multiple projected and scaled copies of the image contained in the reticle. During the exposure process, the wafer stage must track a challenging reference trajectory in all six motion degrees-of-freedom (DoF). The key performance requirement is a synchronized motion between the reticle and the wafer. Indeed, a synchronized motion is essential for avoiding focus and overlay errors. Hence, the true performance criterion is the relative positioning error between the two stages.

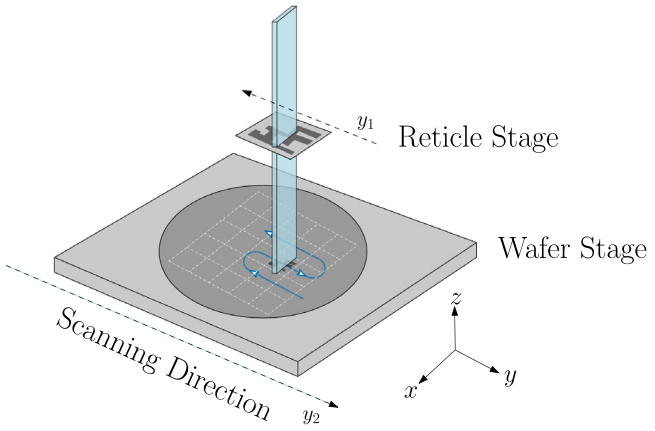

Fig. 2. Abstract representation of the reticle stage and wafer stage. The optical column is disregarded for simplicity. Here, the true performance criterion is the relative error $e_{12} = y_2 - y_1$.

State-of-the-art wafer scanner control

To facilitate development, the wafer stage and reticle stage controllers are designed separately. Here, the control objective is to obtain the smallest tracking error in all six DoF for each of the individual stages. At present, the design of this controller is simplified by applying a decoupling procedure. This allows the use of SISO PID controllers for each of the individual DoF (Butler, 2011). Centralized approaches, including model based $\mathcal{H}_\infty$ robust control (Oomen et al., 2014a; van de Wal et al., 2002) often cannot be justified due to very high modeling requirements. This illustrates that a fully centralized approach for a single subsystem is challenging, moreover, a fully centralized approach encompassing both subsystems, the reticle stage and wafer stage, is infeasible.

Performance limitations introduced by subdivision

At present, decoupling procedures are often used to facilitate SISO controller design for MIMO systems. While this simplifies the control architecture, it also introduces the possibility of performance limitations. This is shown by adopting the case study and constraining it to a single DOF, i.e., both the reticle and wafer stage are considered in the scanning direction only, i.e., along the y-axis as shown in Fig. 2. The control objective is to improve the combined performance of the two stages to best attenuate all disturbances present on both the reticle and wafer stage. To simplify the presentation, two aspects are tacitly omitted from the explanation that are explicitly and appropriately dealt with in the actual implementation. First, both the plant and controller are considered in discrete time, and the framework is tacitly adjusted to this situation. Second, in the waferscanner the reticle stage output is scaled by an optical scaling factor γ that accounts for the optical lens reduction (Butler, 2011). This factor is omitted to facilitate the presentation.

Consider the reticle stage and wafer stage synchronized movement, shown in Fig. 2. Here, the two positioning stages are controlled using a decentralized approach shown in Fig. 3. Here, the problem is restricted to feedback, where stability is a key issue. Feedforward can be directly induced (Oomen, Grassens, & Hendriks, 2015). While the individual stage tracking errors are important and must remain bounded, the true performance criterion is the relative positioning error

$$e_{12} = y_2 - y_1 \tag{1}$$

where y_1 and y_2 are the positions of the first and second positioning stage respectively.

The subsystems shown in Fig. 3 are considered to be approximately decoupled (Stoev, Oomen, & Schoukens, 2016), i.e., it is assumed that there is no interaction between subsystems. An extension that includes this neglected interaction is presented in Section 5. While each of the subsystems typically is controlled in 6 DoF, in the scanning direction the combined system can be modeled as a 2×2 diagonal plant and controller

$$P = \begin{bmatrix} P_1 & 0 \\ 0 & P_2 \end{bmatrix}, \quad K_0 = \begin{bmatrix} C_1 & 0 \\ 0 & C_2 \end{bmatrix}. \tag{2}$$

The main objective is to construct add-on elements to K_0 that maintains the original decentralized controllers C_1, C_2 while improving the overall system performance (1).

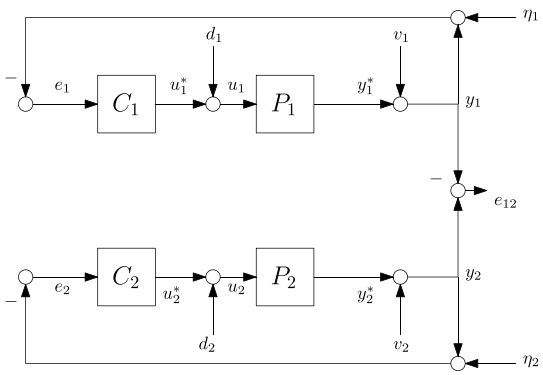

Fig. 3. Decentralized control structure for the double positioning stage system, cast into a disturbance attenuation problem. It is assumed that any referenced induced tracking error is compensated by advanced feed-forward techniques.

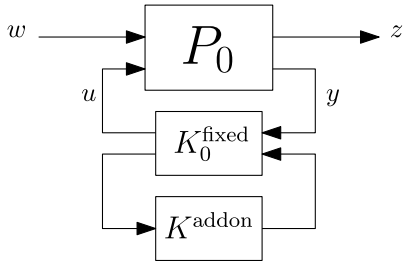

Fig. 4. Standard plant representation, often used in cases where the performance variables z are not equal to the controlled variables y. Here K_0^{fixed} is the fixed diagonal controller in view of Assumption 1 and K^{addon} is the proposed addon controller.

Motivation: beyond traditional performance limitations

The additional add-on controller freedom is used to achieve combined system performance beyond the limitations of the decentralized individual subsystems. One of these limitations is nonminimum-phase (NMP) zeros. If P_1 contains a NMP zero, control performance in this loop is limited, which is directly apparent, e.g., from a Poisson integral relation (Freudenberg et al., 2003), and therefore the overall system performance is limited. Typically, these zeros originate from non-collocated sensor and actuator placement (Hong & Bernstein, 1998) and sampling (Åström, Hagander, & Sternby, 1984).

Further limitations may result from Bandwidth (BW) limitations due to uncertainty or varying dynamics (van Herpen et al., 2014). Typically, the wafer stage can achieve a lower BW compared to the reticle stage. Through the framework developed here, disturbances occurring in one subsystems can be compensated by the other systems in terms of the synchronized motion.

Assumption 1. Throughout, a high performance decentralized, stabilizing controller is assumed to be present and fixed. Such that, if the coupling is disabled then the original system is recovered.

Consider the system in Fig. 3 that is cast into the standard plant in Fig. 4. Here $y = [e_1, e_2]^T$, $u = [u_1, u_2]^T$ and $w = [v_1, v_2]^T$. In addition,

for simplicity $\eta_1 = \eta_2 = d_1 = d_2 = 0$. Next, consider two cases that each define a different performance variable z. In particular z is chosen (1) traditionally $z_1 = [e_1, e_2]^T$ or (2) as is proposed here, $z_2 = e_{12} = [e_1 - e_2]$.

Traditional

The traditional approach is focused on minimizing e_1 and e_2 separately. The controllers C_1 and C_2 are designed accordingly, leading to a closed-loop sensitivity that can be written as

$$\begin{bmatrix} e_1 \\ e_2 \end{bmatrix} = -\underbrace{\begin{bmatrix} S_1 & 0 \\ 0 & S_2 \end{bmatrix}}_{T_{zw_1}} \begin{bmatrix} v_1 \\ v_2 \end{bmatrix}. \tag{3}$$

where S_1 and S_2 are the closed-loop sensitivity functions. As a result, the synchronization error is $e_{12} = S_1 e_1 - S_2 e_2$, and if either P_1 or P_2 contain performance limitations, e.g., NMP zeros, then the synchronization performance is reduced.

Proposed

The central idea is to consider

$$e_{12} = -\begin{bmatrix} I & -I \end{bmatrix} \begin{bmatrix} S_1 & S_{12} \\ S_{21} & S_2 \end{bmatrix} \begin{bmatrix} v_1 \\ v_2 \end{bmatrix} \tag{4}$$

$$= \underbrace{\begin{bmatrix} (S_{21} - S_1) & (-S_{12} + S_2) \end{bmatrix}}_{T_{zw_2}} \begin{bmatrix} v_1 \\ v_2 \end{bmatrix} \tag{5}$$

and to minimize $z_2 = e_{12}$ directly.

The main idea is to design coupling controllers to appropriately shape S_{12} and S_{21}, given the existing decentralized designs. This shows that the performance of the full system in T_{zw_2} is no longer limited by the subsystems, as S_{12} and S_{21} can be used to achieve complementary performance in regions where S_1 and S_2 are limited by, e.g., NMP zeros.

2.2. Requirements

Section 2.1 reveals that controller extension in conjunction with an overall control objective conceptually allows an increase in achievable performance. The main objective of this paper is to improve the synchronized motion of the wafer and reticle stage by designing a framework for add-on controller performance improvement in view of the overall control goal. Fully exploiting this potential in a practically applicable design procedure leads to the following additional requirements.

1. The additional coupling filters must be "add-on" to the existing architecture in view of A1.
2. Nominal stability of the coupled system is guaranteed.
3. Robust stability in the presence of model uncertainty is guaranteed.

The interpretation of the above is the following: Req. 1 ensures that the additional coupling filters do not interfere with the existing decentralized control architecture. Hence, they can be turned off at any time to recover the pre-existing stabilizing feedback controller in Assumption 1 such that the traditional controller design, tuning and implementation can be retained. Moreover, by Req. 2 stability of the original individual subsystems must be guaranteed. Bidirectional coupling leads to potential stability issues (Maciejowski, 1989) hence additional stability requirements should be fulfilled. Finally, Req. 3 is posed such to ensure robust stability of the system under model uncertainties and disturbances. Uncertainties include finite model accuracy, varying plant dynamics, and interaction within and between subsystems.

Achieving performance beyond individual stage limits can be transparently done by connecting the add-on controller freedom with the new performance criterion e_{12}, which is proposed in this paper.

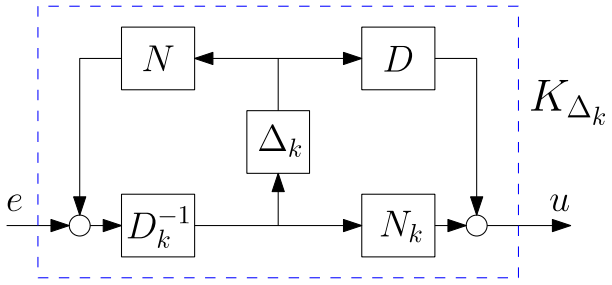

Fig. 5. Controller diagram of a Youla parameterization using coprime factorization. Here, each element is a (2×2) transfer function matrix.

3. Synchronized motion control: Youla framework

Bidirectional coupling leads to inherent two-way interaction and hence system characteristics such as well-posedness and internal stability require a detailed analysis (Maciejowski, 1989). In this section, the standard Youla parameterization is presented that, together with specific choices, leads to the coupling framework that allows systematic coupling of the subsystems while guaranteeing overall system stability. Furthermore, it will be systematically expanded in Section 5 to encompass model uncertainties. Throughout, the subsystems are tacitly assumed scalar and decoupled for clarity and brevity of the exposition. The presented approach directly extends to the MIMO case.

3.1. Standard Youla parameterization

To guarantee nominal stability the Youla parameterization (Anderson, 1998; Youla, Jabr, & Bongiorno, 1976) is employed. Here, the Youla parameterization generates the set of all stabilizing controllers for a nominal system $P_0 \in \mathcal{R}$ as a function of a nominal controller $K_0 \in \mathcal{R}$ and a Youla parameter $\Delta_k \in \mathcal{RH}_\infty$. This allows for direct separation and analysis of the nominal controller K_0 and the additional add-on controller freedom captured by Δ_k. Here, both the nominal controller $K_0 = N_k D_k^{-1}$ and nominal plant $P_0 = N_p D_p^{-1}$ are represented as right-coprime factorizations. The control structure diagram of the Youla parameterization using coprime factorization is shown in Fig. 5.

A right coprime factorization is defined as follows.

Definition 1 (*Right-Coprime Factorization (rcf)*). The ordered pair $\{N, D\}$, with $D \in \mathcal{RH}_\infty^{q\times q}$ and $N \in \mathcal{RH}_\infty^{p\times q}$, is a right-coprime factorization (rcf) of $P \in \mathcal{R}_\infty^{p\times q}$ if

(i) D is invertible (square and non-singular),
(ii) $P = ND^{-1}$,
(iii) N and D are right-coprime.

Here, N and D are right-coprime if there exist matrices $W, L \in \mathcal{RH}_\infty$ such that the Bezout identity (Zhou, Doyle, & Glover, 1996)

$$LN + WD = I, \tag{6}$$

holds. Using the coprime factorizations of the nominal controller and plant, the Youla parameterization provides the set of stabilizing controllers.

Theorem 1 (*Set of Stabilizing Controllers*). *Let $P_0 = N_p D_p^{-1}$ and $K_0 = N_k D_k^{-1}$ where $\{N_p, D_p\}$, $\{N_k, D_K\}$ are rcfs of P_0 and K_0. Let the perturbed controller factors be defined as*

$$N_{k_\Delta} := N_k + D_p \Delta_k, \quad D_{k_\Delta} := D_k - N_p \Delta_k \tag{7}$$

such that

$$K_{\Delta_k} = N_{k_\Delta} D_{k_\Delta}^{-1} \tag{8}$$

where Δ_k is the free Youla parameter. Then it follows that K_{Δ_k} stabilizes P_0 iff $\Delta_k \in \mathcal{RH}_\infty$.

See, e.g., Zhou et al. (1996) for a proof.

3.2. Towards stabilizing bidirectional controller coupling

A bidirectional controller coupling is developed, where closed-loop stability follows through a direct connection to the Youla parameterization. Several specific choices are made that lead to favorable closed-loop system characteristics in view of requirements in Section 2.2. In the common situation where $K_0 \in \mathcal{RH}_\infty$ in industrial applications, then

$$K_0 = \overbrace{\begin{bmatrix} C_1 & 0 \\ 0 & C_2 \end{bmatrix}}^{N_k} \overbrace{\begin{bmatrix} I & 0 \\ 0 & I \end{bmatrix}^{-1}}^{D_k^{-1}}, \tag{9}$$

where C_1, C_2 are the original decentralized controllers, is a suitable RCF. If C_1 or C_2 is unstable or has integral control action, i.e., poles on the imaginary axis, a suitable factorization should be constructed, e.g., Vinnicombe (2000). Similarly, the nominal plant P_0 is written as

$$P_0 = \overbrace{\begin{bmatrix} Z_1 & 0 \\ 0 & Z_2 \end{bmatrix}}^{N_p} \overbrace{\begin{bmatrix} P_1^{-1} Z_1 & 0 \\ 0 & P_2^{-1} Z_2 \end{bmatrix}^{-1}}^{D_p^{-1}}, \tag{10}$$

where Z_1, Z_2 are constructed such that $N_p, D_p \in \mathcal{RH}_\infty$.

Remark 1. The parameterization in (10) is chosen such that Req. 1 is facilitated, other options are possible if improved performance is the sole requirement. However, other filter selections than (10) will not achieve (d) in Theorem 2, which follows below.

For (10) to be a valid coprime factorization as defined in Definition 1, it is required that both P_1, P_2 have no pole/zero cancellations and Z_1, Z_2, which are constructed by the user, should be selected such that they contain no additional RHP zeros other than those required to ensure $D_p \in \mathcal{RH}_\infty$. This is a direct requirement of coprime factorization, since it does not allow for RHP pole/zero cancellation between N_p and D_p^{-1}.

The resulting coupled closed-loop system $\mathcal{F}_l(P_0, K_{\Delta_k})$ can be written as the sum of the original closed-loop system $\mathcal{F}_l(P_0, K_0)$, which is assumed to be stable, and an additional factor that is affine in $\Delta_k \in \mathcal{RH}_\infty$. The design parameters of the add-on coupling controllers are contained in the Youla parameter Δ_k, i.e., define Δ_k as

$$\Delta_k = \begin{bmatrix} 0 & \hat{X} \\ \hat{Y} & 0 \end{bmatrix} \in \mathcal{RH}_\infty. \tag{11}$$

The structure in (11) indicates the structure of the additional coupling between the subsystems. An off-diagonal matrix indicates that there exist only coupling between the subsystems and no coupling within the subsystems, i.e., the decentralized controller is fixed in view of Assumption 1.

Substituting (11) into (7) reveals that the set of stabilizing controllers is given by

$$K_{\Delta_k} = \begin{bmatrix} C_1 & P_1^{-1} Z_1 \hat{X} \\ P_2^{-1} Z_2 \hat{Y} & C_2 \end{bmatrix} \begin{bmatrix} I & -Z_1 \hat{X} \\ -Z_2 \hat{Y} & I \end{bmatrix}^{-1}. \tag{12}$$

Note that $\hat{X}, \hat{Y} \in \mathcal{RH}_\infty$ are the free design parameters, since Z_1, Z_2 must be chosen such that $D_p \in \mathcal{RH}_\infty$.

Remark 2. Note that $K_0 \in \mathcal{RH}_\infty$ and $\Delta_k \in \mathcal{RH}_\infty$ does not immediately imply that $K_{\Delta_k} \in \mathcal{RH}_\infty$. Through a small gain argument, it is sufficient that $\|Z_1 \hat{X} Z_2 \hat{Y}\|_\infty < 1$ to guarantee that $K_{\Delta_k} \in \mathcal{RH}_\infty$ which is often desired for industrial implementation.

3.3. Synchronization framework

By combining the Youla framework in Section 3.1 with the specific choices in Section 3.2, the main result of this section, which constitutes contribution C1, can be stated. The proposed Youla parameterization corresponds to the structure shown in Fig. 6 with $X = Z_1 \hat{X}$ and $Y = Z_2 \hat{Y}$.

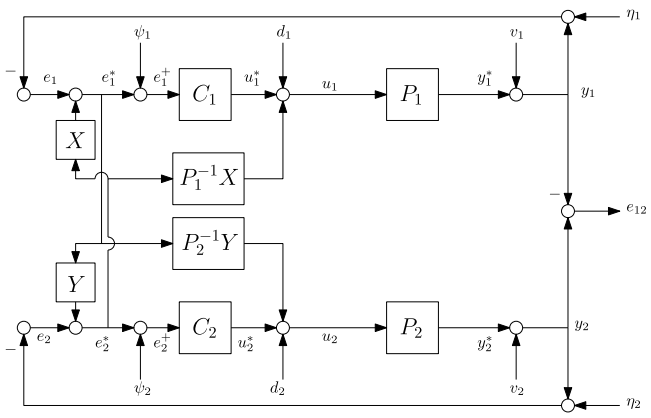

Fig. 6. Proposed controller structure represented in a conventional control block diagram.

By using a specific structure in the coprime factorization of P_0 in (10) the following theorem provides the basis for the design framework, i.e., C1.

Theorem 2 (*Bidirectional Coupling*). *Given the feedback loop with K_0 and system P_0 are defined by (9) and (10), respectively, and Δ_k is chosen as in (11), then the set of stabilizing bidirectional coupling controllers for P_0 is given by:*

$$K_{\Delta_k}(P_0) = \{ N_{k_\Delta} D_{k_\Delta}^{-1} | \Delta_k \in \mathcal{RH}_\infty \} \tag{13}$$

Any controller in (13) then achieves the coupled closed-loop $\mathcal{F}_l(P_0, K_{\Delta_k})$ that has the following properties.

- *(a) $\forall \Delta_k \in \mathcal{RH}_\infty$, $\mathcal{F}_l(P_0, K_{\Delta_k})$ is well-posed and internally stable.*
- *(b) $\forall \Delta_k$, $\mathcal{F}_l(P_0, K_{\Delta_k})$ is affine in Δ_k.*
- *(c) $\forall \Delta_k$, $\mathcal{F}_l(P_0, K_{\Delta_k})_{ii} = \mathcal{F}_l(P_0, K_0)_{ii}$, where $i = [1, 2]$ of each 2×2 block matrix entry.*
- *(d) $\forall \Delta_k$, $e_1^+ \neq f(e_2^+)$ and $e_2^+ \neq f(e_1^+)$, i.e. e_1^+, e_2^+ are invariant to the added coupling.*

See Appendix for a proof.

The above result enables the fulfillment of the requirements posed in Section 2.2. In particular result (a) together with result (b) allows for relatively straightforward tuning of the coupling elements Δ_k and simplifies the nominal stability proof, therefore fulfilling Req. 1. Results (c) and (d) are closely related and reveal that for all Δ_k the coupled closed-loop system maintains the original decentralized controllers. Moreover, the input to the original controllers is solely a function of their respective decentralized loop, i.e., no inter-subsystem coupling is observed and thus Req. 2 is fulfilled. This leaves Req. 3, robust stability, which is addressed in Section 5.

By evaluating the full closed-loop transfer function matrix of the coupled system (A.12) in Appendix a relation for $e_{12} = y_2 - y_1$ can be found. The combined system performance, reduced to a function of two output disturbances v_1, v_2 to facilitate the presentation, is given by

$$e_{12} = -(I + Y) S_1 v_1 + (I + X) S_2 v_2, \tag{14}$$

where $Y = Z_2 \hat{Y}, X = Z_1 \hat{X}$. The structure relates to the result shown in (4). It shows that the coupled system can be described by the original decentralized transfer function matrices and two affine improvement factors $(I + Y), (I + X)$. This is a key result and enables contribution C2 that is presented in Section 4. Therefore, overall superior system performance can be achieved by optimizing the improvement factors under the constraints presented in the Youla framework.

The presented framework is a generalization of previous master–slave type solutions. An unidirectional coupling is most commonly

seen in short-stroke long-stroke master–slave control systems, e.g., in precision actuator design. By setting $Y = 0$, a unidirectional coupling approach as presented, e.g., in Heertjes and Temizer (2012) is recovered as a special case of the presented framework.

4. Design guidelines

In this section, a design procedure to facilitate the design of the add-on controller elements under the constraints of the Youla framework is presented, thereby constituting contribution C2. Perfect disturbance attenuation in (14) is achieved when $X = Y = -I$, i.e., $(I + X) = 0$ and $(I + Y) = 0$. However, this generally leads to an inadmissible coprime factorization in (10), e.g. $D_p \notin \mathcal{RH}_\infty$ caused by non-invertible elements in the nominal plant models of the subsystems. This can be caused by NMP zeros, I/O delay and pole/zero excess, leading to complications with model inversion (Blanken, van de Meijdenberg, & Oomen, 2018).

In the proposed framework the parameters X, Y are constructed out of two components, i.e., $X := Z_1\hat{X}, Y := Z_2\hat{Y}$. Components denoted as Z_1, Z_2 that, in view of requirements, must be chosen such that $\{P_1^{-1}X, P_2^{-1}Y\} \in \mathcal{RH}_\infty$ and components $\hat{X}, \hat{Y}$ that can be designed to minimize e_{12}, where e.g., for the SISO case $|(I + Z_1\hat{X})| < 1$ and $|(I + Z_2\hat{Y})| < 1$, for specific, e.g., low, frequency ranges. Similar approaches for tracking control includes, e.g., Tomizuka (1987).

The following procedure aims to design X, Y such that e_{12} is minimized under the constraints posed by the Youla framework.

Procedure 1: Bidirectional coupling filters.

1: Construct the models P_1, P_2.
2: If $P_1^{-1}, P_2^{-1} \notin \mathcal{RH}_\infty$, construct Z_1, Z_2 such that

$$P_1^{-1}Z_1, P_2^{-1}Z_2 \in \mathcal{RH}_\infty. \tag{15}$$

3: Evaluate

$$|(I + Z_1\hat{X})|, |(I + Z_2\hat{Y})| \; \forall \; \omega \tag{16}$$

and construct $\hat{X}, \hat{Y}$ such that (16) is small for specific, e.g., low-frequency ranges.
4: Implement the stabilizing coupling controller by constructing (13) as described in Theorem 2.

Remark 3. In this section P_1 is used as an example, the design guidelines for P_2 are conceptually similar.

Step 1. Constructing the models for P_1 and P_2 can be done by first principle modeling or parametric model identification procedures. Dealing with a mismatch between the true system and the nominal system models is addressed in Section 5.

Step 2. The NMP zeros of P_1 in (10) are contained in Z_1 such that they cancel in $P_1^{-1}Z_1$. However, this generally makes $Z_1\hat{X} \notin \mathcal{RH}_\infty$ since duplicating the zeros leads to a non-proper filter. Therefore, the NMP elements in Z_1 are constructed as biproper all-pass elements, i.e., their relative degree is 0 and $|Z_1(j\omega)| = 1 \; \forall \; \omega$, to ensure that the parameter $Z_1\hat{X} \in \mathcal{RH}_\infty$ as required by (10). To enforce a proper filter $P^{-1}Z_1$, the element Z_1 includes a low-pass filter with a high-frequency cut-off of order equal to or greater than the amount of pole/zero excess.

Step 3. Using the free design parameter $\hat{X}$, the improvement factor $(I + Z_1\hat{X})$ can be shaped such that the coupled closed-loop disturbance attenuation is improvement at the desired, e.g. low, frequency region. The parameter can be shaped using manual loop-shaping or norm optimal techniques such as $\mathcal{H}_2/\mathcal{H}_\infty-$optimal controller design. If the free design parameter is chosen as $\hat{X} = -I$ it is ensured that $|(I + X)| \ll 1$ at low frequencies which is generally desired for disturbance attenuation.

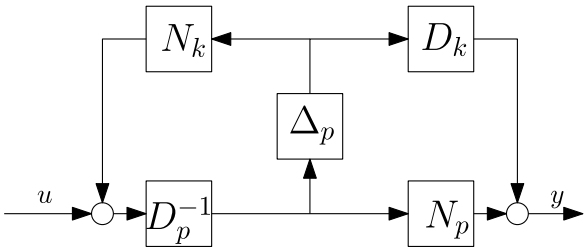

Fig. 7. Dual Youla factorization for a set of stabilized plants $P_{\Delta_p}(K_0)$. Here each of the elements is composed of a 2×2 diagonal transfer function matrix.

Step 4. By following the systematic design procedure the results in Theorem 2 hold, and the stabilizing coupling filter is given by the form in (13).

The guidelines presented in this section facilitate a straightforward manual design of the coupling filters. By following the design rules it is guaranteed that the full system performance is improved, under the assumption that $|(I + Z_1\hat{X})| < 1$ and/or $|(I + Z_2\hat{Y})| < 1$ for some frequency range of interest, while maintaining nominal stability.

Example 1. Consider the following continuous time subsystem model

$$P_1 = \frac{s - a}{s + b},$$

with $a, b \in \mathbb{R} > 0$. The subsystem has a RHP zero and inversion under the constraint in (10) not possible. Therefore, Z_1 is constructed as

$$Z_1 = \frac{s - a}{s + a} \in \mathcal{RH}_\infty.$$

It then follows that

$$P_1^{-1}Z_1 = \frac{s + b}{s + a} \in \mathcal{RH}_\infty,$$

can be used in an admissible RCF in the Youla framework to approximate P_1^{-1}. The improvement factor now becomes

$$(I + Z_1) = I + \frac{s - a}{s + a} \tag{17}$$

of which the amplitude ranges from $|(I + Z_1)| \in [0, 2]$ when $s = j\omega \in [0, \text{inf}]$ due to the phase shift in Z_1.

5. Modeling uncertainty: dual-Youla

This section presents an extension to the Youla framework presented in Section 3 that appropriately addresses robust stability. This is done by extending the Youla framework with a dual-Youla parameterization that facilitates the inclusion of model uncertainties. By extending the framework, robust stability can be guaranteed, constituting contribution C3.

5.1. Dual-Youla

To analyze the effect of model uncertainty on system stability, use is made of a dual-Youla parameterization (Niemann, 2003) as shown in Fig. 7. The parameterization is not unique, but the chosen structure is dual to the framework used to represent nominal bidirectional coupling as presented in Section 3.

Using coprime factorization, it is possible to define a set of plants $P_{\Delta_p}(K_0)$ that are stabilized by a nominal controller K_0.

Theorem 3 (*Set of Stabilized Systems*). *Let P_0 and K_0 have RCF's $P_0 = N_pD_p^{-1}$ and $K_0 = N_kD_k^{-1}$, then the perturbed factors are defined as:*

$$N_{\Delta_p} := N_p + D_k\Delta_p, \quad D_{\Delta_p} := D_p - N_k\Delta_p \tag{18}$$

such that the set of systems that are stabilized by K_0 is equal to

$$P_{\Delta_p}(K_0) = \{N_{\Delta_p}D_{\Delta_p}^{-1} | \Delta_p \in \mathcal{RH}_\infty\}, \tag{19}$$

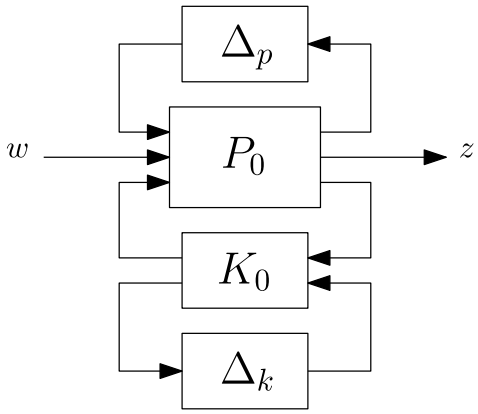

Fig. 8. Standard plant notation of robust bidirectional coupling. The nominal plant and controller are subject to simultaneous perturbations Δ_k and Δ_p respectively.

where set $P_{\Delta_p}(K_0)$ represents all possible systems that are stabilized by the nominal controller K_0 under a model uncertainty Δ_p.

See, e.g., Ma (1988) for a proof.

By using the same coprime factorization for P_0 and K_0 as used in Section 3 the nominal framework is extended to include model uncertainty. In contrast to Δ_k, which is structured to contain only off-diagonal elements, the plant uncertainty model can be unstructured such that

$$\Delta_p := \begin{bmatrix} \Delta_{p_{11}} & \Delta_{p_{12}} \\ \Delta_{p_{21}} & \Delta_{p_{22}} \end{bmatrix} \in \mathcal{RH}_\infty \tag{20}$$

where $\Delta_{p_{11}}, \Delta_{p_{22}}$ indicate nominal subsystem model uncertainty and $\Delta_{p_{12}}, \Delta_{p_{21}}$ indicate (possibly small) inter-subsystem coupling effects.

To construct the subsystem uncertainty model, use is made of a parametric nominal system model and non-parametric system identification measurements (Evers, de Jager, & Oomen, 2018) to significantly reduce modeling effort. By adopting a similar approach as in Oomen et al. (2014a) and van de Wal et al. (2002), where given a measured Frequency Response Function (FRF) P_{frf}, the uncertainty block Δ_k that achieves $P_{frf} = P_{\Delta_k}(K_0)$ is given by:

$$\Delta_k = (D_k + P_{frf} N_k)^{-1}(P_{frf} - P_0)D_p. \tag{21}$$

This provides a straightforward approach to construct the uncertainty model Δ_k using an inexpensive non-parametric estimate of the (MIMO) frequency response function.

Remark 4. Note that $\Delta_k \in \mathcal{RH}_\infty$ as described in Section 3 is fully known. The plant uncertainty model $\Delta_p \in \mathcal{RH}_\infty$, however, is sometimes unknown and can be bounded in $\mathcal{H}_\infty$norm using uncertainty modeling techniques (Oomen et al., 2014b) using closed-loop measurements.

5.2. Double-Youla: robust stability

Using the dual-Youla parameterization in Theorem 3 it is guaranteed that $\forall\ \Delta_p \in \mathcal{RH}_\infty$ the system is stabilized by the nominal controller K_0. Furthermore, by Theorem 1 any K_{Δ_k} induced by $\Delta_k \in \mathcal{RH}_\infty$ stabilizes the nominal plant P_0. In view of C3, the main interest is whether K_{Δ_k} stabilizes all P_{Δ_p} in the closed-loop system $\mathcal{F}_l(P_{\Delta_p}, K_{\Delta_k})$.

By using the result from Theorem 3 the stability proof of the Youla framework can be extended to include the uncertainty model Δ_p such that the following holds

Theorem 4 (*Robust Bidirectional Coupling*)**.** *Consider a closed-loop system $\mathcal{F}_l(P_{\Delta_p}, K_{\Delta_k})$ as shown in Fig. 8, with simultaneous controller Δ_k and plant Δ_p perturbations chosen as (11) and (20), respectively. It can be assumed that $\mathcal{F}_l(P_0, K_0)$ is stable. If the interconnection of Δ_k and Δ_p is stable, then the closed-loop system $\mathcal{F}_l(P_{\Delta_p}, K_{\Delta_k})$ is stable.*

See, e.g., Schrama, Bongers, and Bosgra (1992) and Tay et al. (1998) for a proof. The Youla parameterization for K_{Δ_k} connected with the dual-Youla parameterization for P_{Δ_p} forms the double-Youla parameterization that allows for the full analysis and synthesis of the robust add-on coupling filters.

In the presented framework, the elements Z_1 and Z_2 are fixed by the design guidelines presented Section 4. The elements $\hat{X}, \hat{Y}$ are free design parameters and can be tuned such to achieve performance requirements. These elements $\hat{X}, \hat{Y}$ must be constructed such that the full system $\mathcal{F}_l(P_{\Delta_p}, K_{\Delta_k})$ remains stable. This can be done by two different approaches, manual design and norm-based optimal design

Manual design for RS

Manual loopshaping remains common practice in industry (Oomen, 2018), which motivated the add-on requirement in Section 2.2. And multivariable systems are often decomposed into scalar systems by applying techniques such as sequential loop closing (Maciejowski, 1989, Sec 4.2). Therefore, a suitable stability criterion is required to apply these manual methods to the robust coupling filter design. For this, a stability criterion based on the small gain argument is constructed. Since the coupling filters Δ_k have a clear off-diagonal structure, the structured singular value (Skogestad & Postlethwaite, 2009, Sec 8.8) is used to reduce its conservatism.

Theorem 5. *The closed-loop $\mathcal{F}_l(P_{\Delta_p}, K_{\Delta_k})$ is stable if*

$$\bar{\sigma}(\Delta_k(j\omega)) < \mu_{\Delta_k}(\Delta_p(j\omega))^{-1} \quad \forall\ \omega \tag{22}$$

where $\bar{\sigma}$ denotes the maximum singular value at a single frequency and $\mu_{\Delta_k}(\Delta_p(j\omega))$ denotes the structured singular value of Δ_p with respect to the structure in Δ_k.

Proof. By small-gain argument, Δ_k stabilizes Δ_p if $\|\Delta_k\Delta_p\|_\infty \leq \|\Delta_k\|_\infty\|\Delta_p\|_\infty < 1$. Since $\{\Delta_k, \Delta_p\} \in \mathcal{RH}_\infty$ it holds that $\|\Delta_k\|_\infty\|\Delta_p\|_\infty < 1 \Leftrightarrow \bar{\sigma}(\Delta_k(j\omega))\bar{\sigma}(\Delta_p(j\omega)) < 1\ \forall\ \omega$. And since $\mu_{\Delta_k}(\Delta_p) \leq \bar{\sigma}(\Delta_p)$, Δ_k stabilizes Δ_p if $\bar{\sigma}(\Delta_k(j\omega)) < \mu_{\Delta_k}(\Delta_p)^{-1}\ \forall\ \omega$. Therefore the closed-loop system $\mathcal{F}_l(P_{\Delta_p}, K_{\Delta_k})$ is stable by Theorem 4.

Since it holds that $\mu_{\Delta_k}(\Delta_p) \leq \bar{\sigma}(\Delta_p)$ the criterion in (22) is less conservative than using the regular singular value $\bar{\sigma}$. If no uncertainty is present, i.e., $\Delta_p = 0$, then any $\Delta_k \in \mathcal{RH}_\infty$ is admissible and Theorem 1 is recovered as a special case. A dual result holds for the plant uncertainty Δ_p. The result shows that if (22) holds, then the simultaneous perturbation $\{\Delta_p, \Delta_k\}$ does not induce unstable system behavior. Given that Δ_k is structured as an off-diagonal matrix, and therefore the maximum singular value is determined by the off-diagonal elements, and for robust stability it is required that (22) holds,

$$\{\bar{\sigma}(\hat{X}(j\omega)), \bar{\sigma}(\hat{Y}(j\omega))\} < \mu_{\Delta_k}(\Delta_p(j\omega))^{-1}\ \forall\ \omega \tag{23}$$

is sufficient to achieve robust stability. These bounds can be enforced in arbitrary order, allowing for use of well known manual methods such as sequential loopshaping for the design of the coupling elements $\hat{X}$ and $\hat{Y}$ in Δ_k.

$\mathcal{H}_\infty$-design for RS

An alternative to manual loopshaping design of the coupling filters can be norm-optimal techniques such as $\mathcal{H}_\infty$-design. A one-shot procedure to synthesize Δ_k based weighting filters and Theorem 4 is possible, but complicated due to the structure in Δ_k, e.g., forcing diagonal elements to be zero. This would require techniques such as structured $\mathcal{H}_\infty$ design, see, e.g., Burke, Henrion, Lewis, and Overton (2006). To reduce the computational complexity a different, more traditional $\mathcal{H}_\infty$ approach is taken by applying the sequential stability bounds (23) directly as an $\mathcal{H}_\infty$weighting filter.

The improvement factor $(I + Z_1\hat{X})$, in (14), is represented as a block diagram in Fig. 9. If the parameter $\hat{X}$ is then considered the controller to a plant Z_1 the problem can be rewritten as a standard

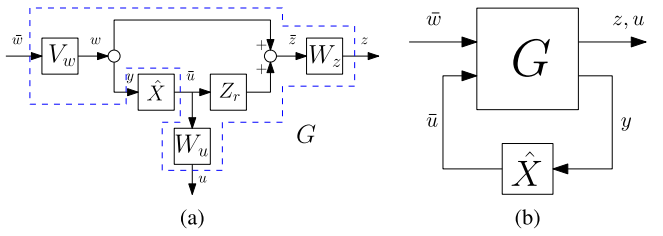

Fig. 9. Block diagram representing the improvement factor, as conventional (a) and standard plant (b).

disturbance attenuation problem in the standard plant shown in Fig. 9 on the right. If $\hat{X}$ and $\hat{Y}$ are bounded by $\mu_{\Delta_k}(\Delta_p(j\omega))^{-1}$ the bidirectional closed-loop system is robustly stable. Since $\{\hat{X}, \hat{Y}\} \in \mathcal{RH}_\infty$ it holds that $\|\hat{X}\|_\infty = \max_\omega \bar{\sigma}(\hat{X}(j\omega))$ and $\|\hat{Y}\|_\infty = \max_\omega \bar{\sigma}(\hat{Y}(j\omega))$. Assuming W_u is a weighting function (van de Wal, van Baars, Sperling, & Bosgra, 2001) on $\hat{X}$ then this yields

$$\|\hat{X}(j\omega)W_u(j\omega)\|_\infty < 1 \tag{24}$$

$$\|\hat{X}(j\omega)\|_\infty < \|W_u(j\omega)^{-1}\|_\infty \tag{25}$$

and if $W_u(j\omega) = \mu_{\Delta_k}(\Delta_p(j\omega))$ this achieves

$$\max_\omega \bar{\sigma}(\hat{X}(j\omega)) < \max_\omega \bar{\sigma}(\mu_{\Delta_k}(\Delta_p(j\omega))^{-1}) \tag{26}$$

and since for a scalar element $\bar{\sigma}(\mu_{\Delta_k}(\Delta_p(j\omega))^{-1}) = \mu_{\Delta_k}(\Delta_p(j\omega))^{-1}$ it fulfills the constraint (23). A similar derivation holds for $\hat{Y}$. Moreover, the output weighting filter W_z is constructed such to achieve the desired performance specification, e.g. $(I + Z_1\hat{X})$ small for low frequencies. The input filter V_w is taken as identity. Using this approach it is possible to automatically synthesis the coupling filters $\hat{X}, \hat{Y}$ to achieve a low-frequency performance improvement while maintaining full system robust stability.

The Double-Youla framework lends itself well to conventional and norm optimal controller synthesis techniques. It allows for the application of the stability criterion separately to each of the coupling filters. And facilitates the controller design engineer to use the preferred tool, e.g., manual loopshaping or norm-based synthesis. This is a useful step towards industrial adaptation, especially since the interconnected multivariable approach is becoming increasingly important in the manufacturing industry while SiSo methods remain the standard (Oomen, 2018).

6. Application to a wafer scanner

The following section applies the developed theoretical framework to the case study presented in Section 2.1 using real system measurements and a high fidelity simulator of an industrial wafer scanner. It illustrates the potential of the framework and constitutes contribution C4.

6.1. Youla framework

To suppress the output disturbance shown in (14) it is desired that the improvement factors are smaller than 1 for low-frequencies up till approximately 200 [Hz].

Applying the nominal design procedure as described in Proc. 1 in Section 4 yields results shown in Fig. 11. It shows the change in the sensitivity function of the disturbance towards the overall performance criterion e_{12}. This change is affine in the improvement factors, shown in Fig. 10, e.g., $(I+Y)S_r$ and $(I+X)S_w$ are the new reticle stage and wafer stage sensitivity functions respectively. Importantly, the dips in the sensitivity functions at higher frequencies are not caused by increased controller gain but rather the improvement factors $(I + X)$ and $(I + Y)$ being locally equal to 0. By applying the additional coupling elements the low-frequency disturbance attenuation is greatly improved.

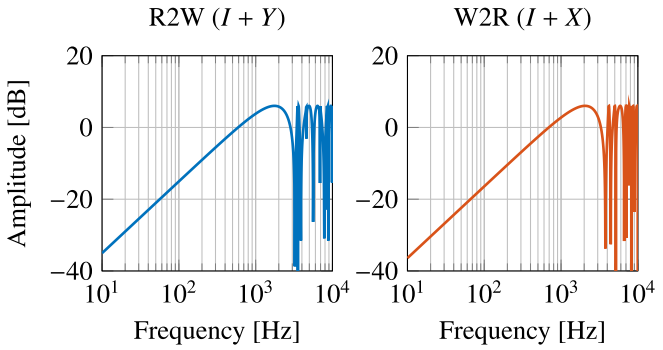

Fig. 10. The improvement factors for R2 W and W2R coupling. It shows that for low frequencies a significant improvement in disturbance attenuation can be achieved.

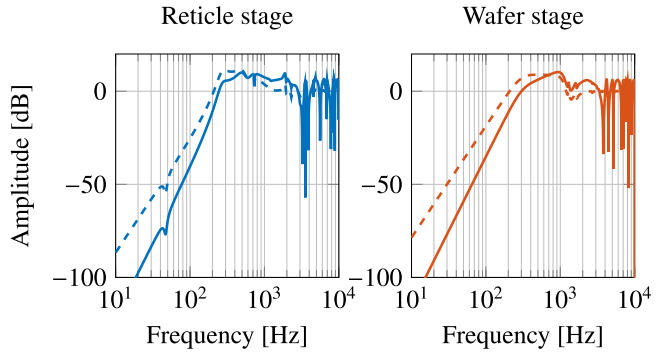

Fig. 11. Original sensitivity for the reticle S_r (- - -) stage and wafer S_w (- - -) stage. Improved reticle sensitivity (——) and wafer sensitivity (——) by applying coupling filter shown in Fig. 10.

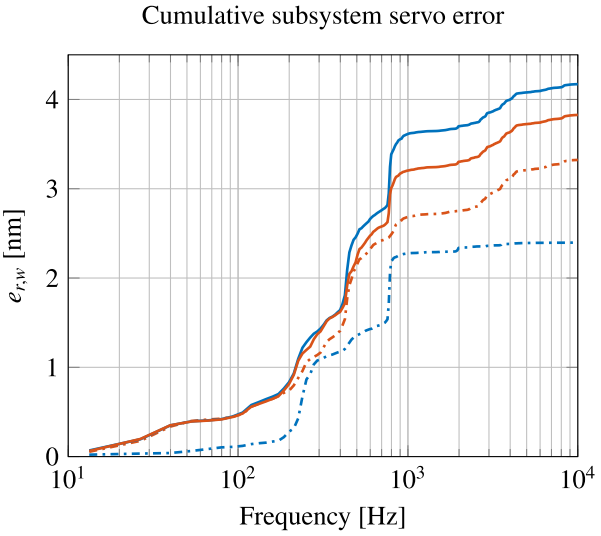

Fig. 12. Cumulative subsystem servo error, mean + 3σ, of the reticle stage (——) and wafer stage (——) with coupling. And the reticle stage (-·-·-) and wafer stage (-·-·-) without coupling. To achieve stage synchronization the reticle stage is synchronized to the wafer stage.

The time domain performance is investigated by utilizing 8 measured servo error traces of wafer scan movement. The expected performance using bidirectional coupling is then simulated using the high fidelity system models in the simulator. The results in Fig. 12 show that at

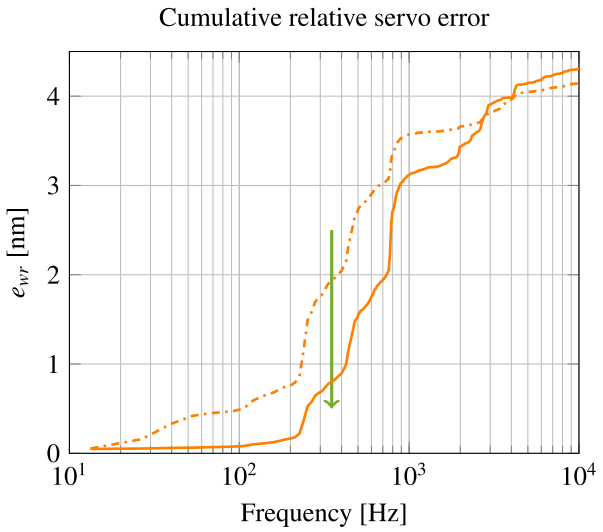

Fig. 13. Cumulative relative servo error with (——) and without (-·-·-) coupling. Results show a clear reduction in low-frequency content at the cost of slight high-frequent deterioration.

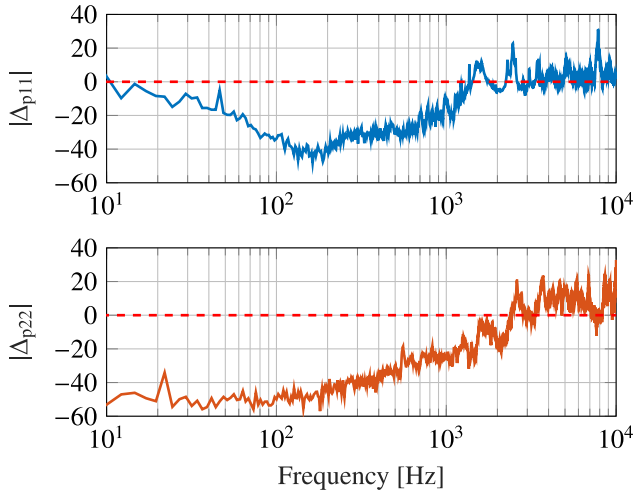

Fig. 14. Maximum uncertainty models for the reticle stage (top) and wafer stage (bottom). Constructed by taking the maximum amplitude over frequency at spatially distributed measurement locations.

low-frequencies the additional controller freedom is exploited to synchronize the stages. The results in Fig. 13 then show that the improved synchronization of the two stages yields a significant improvement in the performance variable e_{12} at low-frequencies.

6.2. Dual youla

The results of the nominal coupling illustrate the potential performance gain by the additional controller freedom. Robust stability under model uncertainty is achieved using the dual Youla result in Section 5. Theorem 1 shows that $\Delta_k \in \mathcal{RH}_\infty$ is sufficient to ensure closed-loop nominal stability. However, this only holds when $\Delta_p = 0$ as shown in Theorem 5. Therefore, to ensure robust stability an uncertainty model is constructed using the nominal plant P_0 and a set of measurements. The uncertainty element is constructed as

$$\Delta_p = \begin{bmatrix} \Delta_{p_{11}} & 0 \\ 0 & \Delta_{p_{22}} \end{bmatrix} \tag{27}$$

where $\Delta_{p_{11}}$ and $\Delta_{p_{22}}$ are constructed by applying (21).

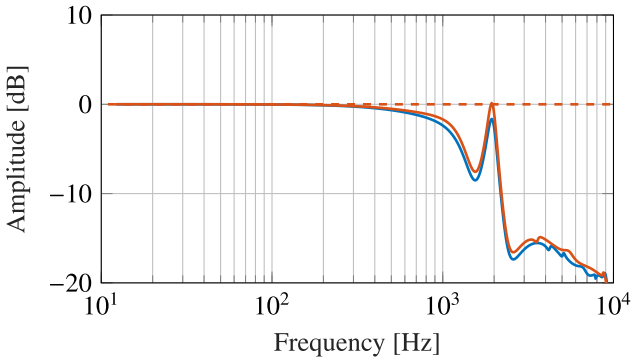

Fig. 15. Robust Youla parameters $\hat{X}$ (——), $\hat{Y}$ (——) compared to the nominal Youla parameters, that are both equal to 0 [dB] (- - -). Phase information is omitted as only the amplitude is used in the small gain analysis.

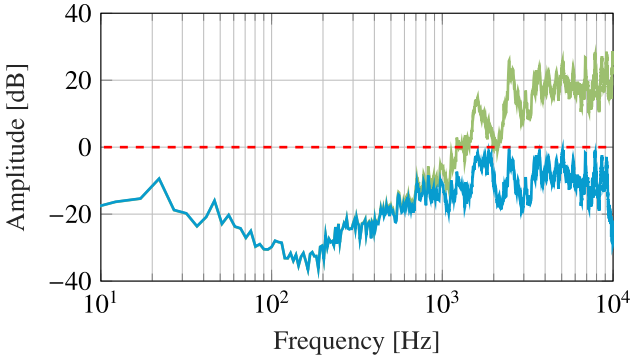

Fig. 16. Small gain criterion using the nominal (——) and newly designed robust (——) Youla parameters. By de-tuning the coupling Δ_k at high frequencies, the small gain criterion using the structured singular value is now fulfilled under the model uncertainty.

The diagonal entries of (27) are shown in Fig. 14, it indicates that at low-frequencies the uncertainty is small since the system dynamics are accurately modeled by a rigid body approximation. At higher frequencies the nominal system model contains a relatively large amount of uncertainty. This increase in model uncertainty limits the amount of coupling admissible by 5. Moreover, the results in Fig. 16 show that the system is not guaranteed to be stable as (22) is not fulfilled. To achieve robust stability, $\mathcal{H}_\infty$-synthesis, following Theorem 5, robust coupling filters are synthesized. The new Youla parameters are shown in Fig. 15. Robust stability is achieved by including high-frequency roll-off, thus limiting the coupling in regions with high model uncertainty as shown in Fig. 14. The results in Fig. 16 show that using the new coupling elements, under Theorem 5 the system is now robustly stable.

6.3. Results

Fig. 17 compares the closed-loop disturbance rejection using either the nominal or robust coupling filters. It shows that a slight low-frequency performance deterioration is required to enable sufficient robustness against the large model uncertainty at high-frequencies.

The results in Table 1 present the averaged time-domain scanning results at 5 distributed locations on the wafer and 3σ indicates the 99.73% confidence interval. It shows that a decrease in Moving Average (MA), which is correlated to overlay and the more critical performance indicator, causes an increased Moving Standard Deviation (MSD), which is correlated to image focus (Butler, 2011). And that by adding robustness to the nominal coupling filters some performance is lost. However, both the nominal and robust coupling achieve a significant reduction in MA and therefore yield superior overlay performance.

Table 1
MA and MSD results using nominal or robust coupling filters.

	No coupling	Nominal	Robust
MA [pm]			
3σ	565	108	200
Peak	603	182	338
MSD [pm]			
3σ	2879	3329	3304
Peak	3145	3485	3670

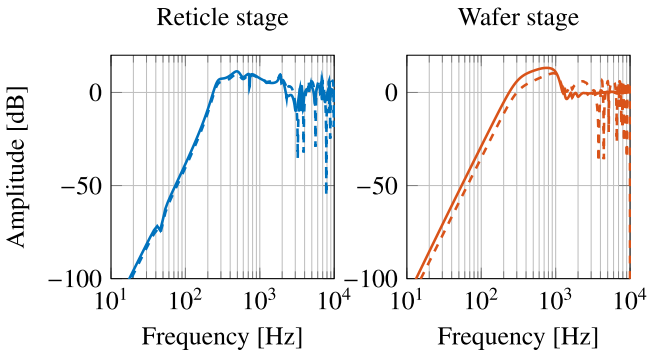

Fig. 17. Bode magnitude diagram comparing the sensitivity using nominal coupling, for the reticle stage (- - -) and wafer stage (- - -), and robust coupling, for the reticle stage (——) and wafer stage (——).

7. Conclusion

The framework presented in this paper enables coupling of subsystems to improve overall system performance. The framework is well-suited for a large range of mechatronic systems, where subsystems are often designed, built, and controlled separately. The proposed framework enables a systematic performance improvement of the integrated system.

A nominal design approach is given where the coupled system behavior is expressed as a straightforward combination of the original closed-loop characteristics and an affine factor, allowing for simplified design. Model uncertainty is appropriately addressed and a sufficient condition for robust stability is provided that can be used in a posteriori analysis or a priori constraint based $\mathcal{H}_\infty$-synthesis of the add-on coupling elements. This in contrast to the industry standard of manual tuning that requires significant trial and error by an experienced control engineer. This substantially simplifies the process of coupling an increasing amount of subsystems contained in modern systems-of-systems used in the manufacturing industry. The resulting design framework facilitates improved overall system performance and achieves robust stability. In addition, there is current research effort aiming to employ the developed framework for the coupling of thermo-mechanical systems (Evers et al., 2018), for real-time thermal induced deformation compensation.

Acknowledgments

This work is supported by the Advanced Thermal Control consortium, ASML research, and is part of the research programme VIDI with project number 15698, which is (partly) financed by the Netherlands Organization for Scientific Research (NWO). The authors thank ASML research for the fruitful collaboration.

Appendix. Proof of Theorem 2

Proof. Following Schrama et al. (1992), the set of stabilizing controllers is defined using the perturbed controller factors:

$$N_{k_\Delta} := N_k + D\Delta_k, \quad D_{k_\Delta} := D_k - N\Delta_k \tag{A.1}$$

These factors, under the controller and plant definition given in Theorem 2, are equal to

$$N_{k_\Delta} = \begin{bmatrix} C_1 & 0 \\ 0 & C_2 \end{bmatrix} + \begin{bmatrix} P_1^{-1}Z_1 & 0 \\ 0 & P_2^{-1}Z_2 \end{bmatrix} \Delta_k, \tag{A.2}$$

$$D_{k_\Delta} = \begin{bmatrix} I & 0 \\ 0 & I \end{bmatrix} - \begin{bmatrix} Z_1 & 0 \\ 0 & Z_2 \end{bmatrix} \Delta_k. \tag{A.3}$$

If it is then defined that Δ_k equals

$$\Delta_k = \begin{bmatrix} 0 & \hat{X} \\ \hat{Y} & 0 \end{bmatrix} \tag{A.4}$$

the perturbed controller factors become

$$N_{k_\Delta} = \begin{bmatrix} C_1 & P_1^{-1}Z_1\hat{X} \\ P_2^{-1}Z_2\hat{Y} & C_2 \end{bmatrix}, D_{k_\Delta} = \begin{bmatrix} I & -Z_1\hat{X} \\ -Z_2\hat{Y} & I \end{bmatrix} \tag{A.5}$$

thus yielding

$$K_{\Delta_k}(P_0) = \begin{bmatrix} C_1 & P_1^{-1}X \\ P_2^{-1}Y & C_2 \end{bmatrix} \begin{bmatrix} I & -X \\ -Y & I \end{bmatrix}^{-1} \tag{A.6}$$

where $X = Z_1\hat{X}$ and $Y = Z_2\hat{Y}$. The closed-loop equations are derived by using that $y = (I + P_0K_{\Delta_k}(P_0))^{-1}\tilde{e}$, which brings the full closed loop to

$$\begin{bmatrix} y_1 \\ y_2 \end{bmatrix} = \underbrace{\left(\begin{bmatrix} I & 0 \\ 0 & I \end{bmatrix} + \begin{bmatrix} P_1C_1 & P_1P_1^{-1}X \\ P_2P_2^{-1}Y & P_2C_2 \end{bmatrix} \underbrace{\begin{bmatrix} I & -X \\ -Y & I \end{bmatrix}^{-1}}_{H^{-1}} \right)}_{M^{-1}} \tilde{e} \tag{A.7}$$

where

$$\tilde{e} = \left(\begin{bmatrix} v_1 + P_1d_1 + P_1C_1\psi_1 \\ v_2 + P_2d_2 + P_2C_2\psi_2 \end{bmatrix} - \begin{bmatrix} P_1C_1 & P_1P_1^{-1}X \\ P_2P_2^{-1}Y & P_2C_2 \end{bmatrix} \begin{bmatrix} I & -X \\ -Y & I \end{bmatrix}^{-1} \begin{bmatrix} \eta_1 \\ \eta_2 \end{bmatrix} \right) \tag{A.8}$$

Here, H^{-1} is written, using block matrix inverse (Lu & Shiou, 2002), as

$$H^{-1} = \begin{bmatrix} \alpha & X\beta \\ Y\alpha & \beta \end{bmatrix} \tag{A.9}$$

where $\alpha = (I - XY)^{-1}$ and $\beta = (I - YX)^{-1}$, yielding

$$M = \begin{bmatrix} I + (XY + P_1C_1)\alpha & (P_1C_1 + I)X\beta \\ (P_2C_2 + I)Y\alpha & I + (YX + P_2C_2)\beta \end{bmatrix} \tag{A.10}$$

where entries $M(1,1)$ and $M(2,2)$ can be simplified by using $I = \alpha^{-1}\alpha$ and $I = \beta^{-1}\beta$ respectively. This brings M to

$$M = \begin{bmatrix} (I + P_1C_1)\alpha & (I + P_1C_1)X\beta \\ (I + P_2C_2)Y\alpha & (I + P_2C_2)\beta \end{bmatrix} \tag{A.11}$$

Using the block matrix inverse together with the matrix identity $(AB)^{-1} = B^{-1}A^{-1}$, it is found that

$$M^{-1} = \begin{bmatrix} (I + P_1C_1)^{-1} & -\alpha^{-1}X\beta(I + P_2C_2)^{-1} \\ -\beta^{-1}Y\alpha(I + P_1C_1)^{-1} & (I + P_2C_2)^{-1} \end{bmatrix}. \tag{A.13}$$

Using the push-through rule (Skogestad & Postlethwaite, 2009, p65) $(I + AB)^{-1}A = A(I + BA)^{-1}$ it is seen that $X\beta = X(I - YX)^{-1} =$

$$\begin{bmatrix} y_1 \\ y_2 \\ \hline e_1 \\ e_2 \\ \hline e_1^+ \\ e_2^+ \\ \hline u_1 \\ u_2 \\ \hline e_{12} \end{bmatrix} = \left[\begin{array}{cc|cc|cc|cc} S_1 & -XS_2 & PS_1 & -XPS_2 & T_1 & -XT_2 & -T_1 & -XS_2 \\ -YS_1 & S_2 & -YPS_1 & PS_2 & -YT_1 & T_2 & -YS_1 & -T_2 \\ \hline -S_1 & XS_2 & -PS_1 & XPS_2 & -T_1 & XT_2 & -S_1 & XS_2 \\ YS_1 & -S_2 & YPS_1 & -PS_2 & YT_1 & -T_2 & YS_1 & -S_2 \\ \hline -S_1 & 0 & -PS_1 & 0 & S_1 & 0 & -S_1 & 0 \\ 0 & -S_2 & 0 & -PS_2 & 0 & S_2 & 0 & -S_2 \\ \hline CS_1 & P_1^{-1}XS_2 & S_1 & -P_1^{-1}XSP_2 & CS_1 & -P_1^{-1}XT_2 & CS_1 & P_1^{-1}XS_2 \\ P_2^{-1}YS_1 & CS_2 & -P_2^{-1}YSP_1 & S_2 & -P_2^{-1}YT_1 & CS_2 & P_2^{-1}YS_1 & CS_2 \\ \hline -(I+Y)S_1 & (I+X)S_2 & -(I+Y)PS_1 & (I-X)PS_2 & -(I+Y)T_1 & (I-X)T_2 & -YS_1+T_1 & -T_2+XS_2 \end{array}\right] \begin{bmatrix} v_1 \\ v_2 \\ \hline d_1 \\ d_2 \\ \hline \psi_1 \\ \psi_2 \\ \hline \eta_1 \\ \eta_2 \end{bmatrix} \tag{A.12}$$

Box I.

$(I - XY)^{-1}X = \alpha X$ which brings M^{-1} to

$$M^{-1} = \begin{bmatrix} (I + P_1C_1)^{-1} & -X(I + P_2C_2)^{-1} \\ -Y(I + P_1C_1)^{-1} & (I + P_2C_2)^{-1} \end{bmatrix} \tag{A.14}$$

The full closed-loop transfer function matrix is derived by repeating the steps for all disturbances and it is provided in (A.12).

(a) Evaluating all entries of the matrix (A.12) is sufficient (Zhou et al., 1996) to guarantee well-posedness and internal stability under the assumption that $\Delta_k \in \mathcal{RH}_\infty$.

(b) Matrix (A.12) is clearly affine in Δ_k.

(c) For each of the (2×2) block matrices in (A.12) the diagonal entries are those of the original closed-loop system.

(d) By evaluating the 5th and 6th row of (A.12) it is seen that there is no interaction since the off-diagonals are 0.

References

Anderson, B. D. (1998). From Youla–Kucera to identification, adaptive and nonlinear control. *Automatica*, *34*(12), 1485–1506. http://dx.doi.org/10.1016/S0005-1098(98)80002-2.

Åström, K., Hagander, P., & Sternby, J. (1984). Zeros of sampled systems. *Automatica*, *20*(1), 31–38. http://dx.doi.org/10.1016/0005-1098(84)90062-1.

Barton, K. L., & Alleyne, A. G. (2007). Cross-coupled ILC for improved precision motion control: Design and implementation. In *American control conference, 2007. ACC'07* (pp. 5496–5502).

Blanken, L., van de Meijdenberg, I., & Oomen, T. (2018). Inverse system estimation for feedforward: A kernel-based approach for non-causal systems. In *18th IFAC symposium on system identification* (pp. 1050–1055). Stockholm, Sweden.

Boeren, F., Bruijnen, D., van Dijk, N., & Oomen, T. (2014). Joint input shaping and feedforward for point-to-point motion: Automated tuning for an industrial nanopositioning system. *Mechatronics*, *24*(6), 572–581. http://dx.doi.org/10.1016/j.mechatronics.2014.03.005.

Bolder, J. (2015). *Flexibility and robustness in iterative learning control : With applications to industrial printers*. (Ph.D. thesis), Eindhoven University of Technology.

Burke, J. V., Henrion, D., Lewis, A. S., & Overton, M. L. (2006). HIFOO - A MATLAB package for fixed-order controller design and H-infinity optimization. In *5th IFAC symposium on robust control design*, Toulouse, France.

Butler, H. (2011). Position control in lithographic equipment [applications of control]. *IEEE Control Systems*, *31*(5), 28–47.

Chen, Z., He, J., Zheng, Y., Song, T., & Deng, Z. (2016). An optimized feedforward decoupling PD register control method of roll-to-roll web printing systems. *IEEE Transactions on Automation Science and Engineering*, *13*(1), 274–283. http://dx.doi.org/10.1109/TASE.2015.2489687.

Chen, X., Jiang, T., & Tomizuka, M. (2015). Pseudo Youla–Kucera parameterization with control of the waterbed effect for local loop shaping. *Automatica*, *62*, 177–183. http://dx.doi.org/10.1016/j.automatica.2015.09.029.

Evers, E., de Jager, B., & Oomen, T. (2018). Improved local rational method by incorporating system knowledge: with application to mechanical and thermal dynamical systems. In *18th IFAC symposium on system identification, SYSID 2018* (pp. 808–813). Stockholm, Sweden.

Evers, E., van de Wal, M., & Oomen, T. (2017). Synchronizing decentralized control loops for overall performance enhancement: A Youla framework applied to a wafer scanner. In *IFAC world congress* (pp. 11332–11337).

Freudenberg, J., Hollot, C., Middleton, R., & Toochinda, V. (2003). Fundamental design limitations of the general control configuration. *IEEE Transactions on Automatic Control*, *48*(8), 1355–1370. http://dx.doi.org/10.1109/TAC.2003.815017.

de Gelder, E., van de Wal, M., Scherer, C., Hol, C., & Bosgra, O. (2006). Nominal and robust feedforward design with time domain constraints applied to a wafer stage. *Journal of Dynamic Systems, Measurement, and Control*, *128*(2), 204. http://dx.doi.org/10.1115/1.2192821.

Heertjes, M., & Temizer, B. (2012). Data-based control tuning in master-slave systems. In *American control conference (ACC), 2012* (pp. 2461–2466). IEEE.

van Herpen, R., Oomen, T., Kikken, E., van de Wal, M., Aangenent, W., & Steinbuch, M. (2014). Exploiting additional actuators and sensors for nano-positioning robust motion control. *Mechatronics*, *24*(6), 619–631.

Hong, J., & Bernstein, D. S. (1998). Bode integral constraints, collocation, and spillover in active noise and vibration control. *IEEE Transactions on Control Systems Technology*, *6*(1), 111–120.

Jabben, L., Trumper, D., & Eijk, J. v. (2008). Dynamic error budgeting - an integral system design oppoach for high precision machines. (pp. 363–367). Bedford: Euspen.

Lambregts, C. J., Heertjes, M. F., & van der Veek, B. J. (2015). Multivariable feedback control in stage synchronization. In *American control conference, ACC, 2015* (pp. 4149–4154). IEEE.

Lu, T. T., & Shiou, S. H. (2002). Inverses of 2 × 2 block matrices. *Comput. Math. Appl.*, *43*(1–2), 119–129. http://dx.doi.org/10.1016/S0898-1221(01)00278-4.

Ma, C. (1988). Comments on "A necessary and sufficient condition for stability of a perturbed system" by Q. Huang and R. Liu. *IEEE Transactions on Automatic Control*, *33*(8), 796–797. http://dx.doi.org/10.1109/9.1305.

Maciejowski, J. M. (1989). Multivariable feedback design. In *Electronic systems engineering series*. Wokingham, England: Addison-Wesley.

Mishra, S., Yeh, W., & Tomizuka, M. (2008). Iterative learning control design for synchronization of wafer and reticle stages. In *American control conference, 2008* (pp. 3908–3913). IEEE.

Navarrete, M. O., Heertjes, M. F., & Schmidt, R. H. M. (2015). Common zeros in synchronization of high-precision stage systems. In: *Mechatronics, ICM, 2015 IEEE international conference on*, (pp. 602–607).

Niemann, H. (2003). Dual Youla parameterisation. *IEE Proceedings - Control Theory and Applications*, *150*(5), 493–497. http://dx.doi.org/10.1049/ip-cta:20030685.

Oomen, T. (2018). Advanced motion control for precision mechatronics: Control, identification, and learning of complex systems. *IEEJ Journal of Industry Applications*, *7*(2), 127–140. http://dx.doi.org/10.1541/ieejjia.7.127.

Oomen, T., Grassens, E., & Hendriks, F. (2015). Inferential motion control: Identification and robust control framework for positioning an unmeasurable point of interest. *IEEE Transactions on Control Systems Technology*, *23*(4), 1602–1610. http://dx.doi.org/10.1109/TCST.2014.2371830.

Oomen, T., van Herpen, R., Quist, S., van de Wal, M., Bosgra, O., & Steinbuch, M. (2014a). Connecting system identification and robust control for next-generation motion control of a wafer stage. *IEEE Transactions on Control Systems Technology*, *22*(1), 102–118. http://dx.doi.org/10.1109/TCST.2013.2245668.

Oomen, T., van der Maas, R., Rojas, C. R., & Hjalmarsson, H. (2014b). Iterative data-driven H norm estimation of multivariable systems with application to robust active vibration isolation. *IEEE Transactions on Control Systems Technology*, *22*(6), 2247–2260. http://dx.doi.org/10.1109/TCST.2014.2303047.

Prempain, E., Turner, M. C., & Postlethwaite, I. (2009). Coprime factor based anti-windup synthesis for parameter-dependent systems. *Systems & Control Letters*, *58*(12), 810–817. http://dx.doi.org/10.1016/j.sysconle.2009.09.002.

Sakata, K., & Fujimoto, H. (2009). Master-slave synchronous position control for precision stages based on multirate control and dead-time compensation. In *Advanced intelligent mechatronics, 2009. AIM 2009. IEEE/ASME international conference on* (pp. 263–268). IEEE.

Schrama, R. J., Bongers, P. M., & Bosgra, O. H. (1992). Robust stability under simultaneous perturbations of linear plant and controller. In *Decision and control, 1992., proceedings of the 31st IEEE conference on* (pp. 2137–2139). IEEE.

Seron, M., Braslavsky, J., & Goodwin, G. C. (1997). Fundamental limitations in filtering and control. In *Communications and control engineering*. London; New York: Springer.

Skogestad, S., & Postlethwaite, I. (2009). Multivariable feedback control: Analysis and design, 2nd ed., Chichester: Wiley.

Stoev, J., Oomen, T., & Schoukens, J. (2016). Tensor methods for MIMO decoupling using frequency response functions. *IFAC-PapersOnLine*, *49*(21), 447–453. http://dx.doi.org/10.1016/j.ifacol.2016.10.644.

Tay, T. T., Mareels, I., & Moore, J. B. (1998). *High performance control*. Springer Science & Business Media.

Tomizuka, M. (1987). Zero phase error tracking algorithm for digital control. *Journal of Dynamic Systems, Measurement, and Control*, *109*(1), 65. http://dx.doi.org/10.1115/1.3143822.

Vinnicombe, G. (2000). Uncertainty and feedback - H_{∞} loop-shaping and the v-Gap metric. Imperial College Press, http://dx.doi.org/10.1142/9781848160453.

van de Wal, M., van Baars, G., Sperling, F., & Bosgra, O. (2001). Experimentally validated multivariable/spl mu/feedback controller design for a high-precision wafer stage. In *Decision and control, 2001. Proceedings of the 40th IEEE conference on: Vol. 2*, (pp. 1583–1588). IEEE.

van de Wal, M., van Baars, G., Sperling, F., & Bosgra, O. (2002). Multivariable feedback control design for high-precision wafer stage motion. *Control Engineering Practice*, *10*(7), 739–755. http://dx.doi.org/10.1016/S0967-0661(01)00166-6.

Wang, C., Yin, W., & Duan, G. (2006). Cross-coupling control for synchronized scan of experimental wafer and reticle stage. In *Technology and innovation conference, 2006. ITIC 2006. International* (pp. 1168–1172). IET.

Youla, D., Jabr, H., & Bongiorno, J. (1976). Modern Wiener-Hopf design of optimal controllers–Part II: The multivariable case. *IEEE Transactions on Automatic Control*, *21*(3), 319–338.

Zhou, K., Doyle, J. C., & Glover, K. (1996). *Robust and optimal control*. Upper Saddle River, N.J: Prentice Hall.

van Zundert, J., Luijten, F., & Oomen, T. (2018). Achieving perfect causal feedforward control in presence of nonminimum-phase behavior: Exploiting additional actuators and squaring down. In *2018 IEEE American control conference*, Milwaukee, Wisconsin.